



Morphology control of hydroxyapatite microcrystals: Synergistic effects of citrate and CTAB



Hui Yang^a, Yingjun Wang^{b,*}

^a School of Materials Science and Engineering, Jiangxi University of Science and Technology, Ganzhou 341000, China

^b School of Materials Science and Engineering, South China University of Technology, Guangzhou 510641, China

ARTICLE INFO

Article history:

Received 23 November 2015

Received in revised form 8 January 2016

Accepted 20 January 2016

Available online 22 January 2016

Keywords:

Hydroxyapatite

Microcrystals

Hierarchical structure

Citrate

CTAB

ABSTRACT

Using hydrothermal treatment and with the synergistic regulating effects of citrate and CTAB, various 3D hierarchical superstructure of hydroxyapatite (HAp) microcrystals were synthesized by simply adjusting the Ct/CTAB ratio and calcium–citrate complex (CC) morphology. The resulting superstructure was characterized using X-ray diffraction (XRD), Fourier Transform infrared spectroscopy (FTIR), field-emission scanning electron microscopy (FESEM) etc. With the shape transformation of CC from sphere-like colloid, nano-needle to lamellar-like particles, the final products were hollow spheres, bunched-like microrods and nanorod clusters, respectively. A possible mechanism for the formation of HAp hierarchical microstructure was proposed.

© 2016 Elsevier B.V. All rights reserved.

1. Introduction

Due to the composition similarity to the natural minerals of calcified tissue, HAp possesses excellent biocompatibility and osteoconductivity, and has been widely used in medical, biological and other fields [1,2]. Till now, HAp has been synthesized by diverse chemical-processing routes, such as chemical precipitation, emulsion technique, hydrothermal treatment, milling approach and so on [3–6]. However, as taking account of the relationship between structure and properties, some complex structures, which are organized by nanoscale building blocks being self-assembled into 2D or even 3D structure, can't be easily attained by a simple method without the aid of additives. Hence, how to control the self assembly of HAp nanoparticles is becoming an increasingly hot topic. To date, many additives have been found to successfully modify the structure of HAp crystals [7].

The excellent properties of nature tissue with simple composition are credited with their complex architecture, which inspired abundant researchers to study their formation mechanism. It is shared that the ordered structures in mineralized tissues originate from assemblies of biomacromolecules, such as protein, polysaccharides etc. For instance, collagen regulates the growth, morphology, and structure of mineral phase [8]. Most carboxylate-rich proteins promote nucleation of minerals by decreasing the induction time [9]. Other than biomacromolecules, the biomicromolecules are regarded as another important factor in biominer-alization process. Trisodium citrate, a common bioorganic micro-

molecule involved in many biological cycles, plays an important role in bone resorption, apatite formation in tooth enamel, and nucleation, thickening nano-size stabilization of HAp crystallites in bone [10,11]. In synthesis field, citrate is widely used as an additive in the synthesis of single crystals, colloid particles, inorganic/organic complex and nanoparticles with fine structure and excellent properties [12,13]. In addition, large amount of synthesized organic additives are used in regulating the formation of inorganic particles. Hexadecyltrimethylammonium bromide (CTAB) is an ordinary surfactant and extensively being used for synthesizing nanoparticles [14,15].

Herein, inspired by the role of Ct and CTAB in biominer-alization and particle synthesis process, both of them were used to synergistically regulate the nucleation and crystal growth of HAp. Varied a range of parameters were carefully investigated, and results showed that the ratio of Ct/CTAB and the initial status of citrate calcium (CC) played important role in regulating the structure of the final products. In addition, to demonstrate the interaction among Ct, CTAB and HAp crystals, a possible modifying mechanism was proposed.

2. Experimental section

2.1. Materials

All chemicals were analytically pure and purchased from Guangzhou Chemical Corporation. Unless otherwise indicated, all of the preparation processes were conducted at room temperature. In brief, 0.805 g trisodium citrate dihydrate (Ct) and 0.47 g $\text{Ca}(\text{NO}_3)_2 \cdot 4\text{H}_2\text{O}$ were dissolved in 15 ml deionized water, and stirred for 12 h to form solution

* Corresponding author.

E-mail addresses: yanghui_2521@163.com (H. Yang), imwangyj@163.com (Y. Wang).

A. 0.2 g CTAB, 0.16 g $(\text{NH}_4)_2\text{HPO}_4$ were dissolved in 20 ml deionized water, and then its pH was adjusted to 5 with 2 M HNO_3 to form solution B. Solution A was dropwise introduced into solution B under vigorous stirring using a magnetic stirrer, the corresponding mole ratio of Ct/CTAB was 5/1, the Ct/CTAB ratio was adjusted by changing Ct's mass, and remained CTAB's mass constant. Then the mixture solution was transferred to a Teflon bottle with a volume of 100 ml, placed into a stainless steel autoclave, then sealed and maintained at 180 °C for 24 h. After the autoclave cooled to room temperature naturally, the precipitation was washed with deionized water and ethanol three times, respectively, and then centrifuged and freeze dried. The shape transformation of CC was studied as follows. 0.483 g Ct and 0.47 g $\text{Ca}(\text{NO}_3)_2 \cdot 4\text{H}_2\text{O}$ were dissolved in 15 ml deionized water, and stirred for a certain time (10–60 min), the products were adsorbed onto a copper grids by immersing the grids into the solution for 15 s, then blotted with filter paper to remove excess solution, the grids were then dried naturally at room temperature. At the same time, the precipitate was centrifuged and washed with de-ionized water several times, then freeze dried for further characterizations. Besides, the effects of CC's shape transformation on the final structure of HAp were investigated, the Ct/CTAB ration kept at 3/1, and the stirring time of solution A was altered from 10 min to 120 min, the following preparation processes were the same as that of HAp prepared at different Ct/CTAB ratio condition.

2.2. Characterization

The final crystals were characterized by field emission scanning electron microscopy (FESEM) on a Nova NanoSEM 430 (FEI, Netherlands) microscope. Transmission Electron Microscope (TEM) was performed using JEOL JEM-2100 with a field emission gun operating at 200 kV. Images were acquired digitally on a Gatan 832 CCD camera. Powder X-ray diffraction (XRD) patterns were recorded on a PANalytical X'Pert PRO

diffractometer with $\text{Cu K}\alpha$ ($\lambda = 0.15418 \text{ nm}$) radiation, and the XRD data were collected between 10° to 70° in an interval of 0.02° with the scanning rate at 1°/min. Fourier Transform Infra-Red (FT-IR) spectra were obtained in the range of 400–4000 cm^{-1} using Bruker vector 33 with a resolution of 0.3 cm^{-1} . TG measurements were performed using STA 449C (Netsch, German).

3. Results and discussion

A series of experiments were conducted at different Ct/CTAB mole ratio. As shown in Fig. 1, low Ct/CTAB ratio led to the formation of HAp microspheres, these microspheres were composed by nanorods, which were closely and orderly compact perpendicular to its surface, the morphology of the products was uniform and their diameter was about 4 μm . Then the morphology uniformity changed gradually as the corresponding ratio increased, some tiny clusters composed by nanorods with diameter of ~2 μm formed (Fig. 1(b)), and microspheres formed at low ratio condition disappeared (Fig. 1(c)). Further, increasing the Ct/CTAB ratio led to the shape transformation of microparticles' building blocks from nanorods to nano-needle, and the final product were nano-needle clusters. As the Ct/CTAB ratio came to 1/1, microflakes with diameter of ~2 μm formed, most of them were dispersive, while a small number of them aggregated orderly and generated unstable sphere-like clusters (Fig. 1(e)). A control group without adding CTAB was performed, and the results showed that the final products were microspheres composed by microflakes perpendicular to its surface, the size of microsphere was about 50 μm . After a short time ultrasonic dispersing treatment, the microsphere structure collapsed easily, hence, there were many dispersive flasks like particles.

XRD patterns of the as-prepared samples were shown in Fig. 2. Results showed that different Ct/CTAB ratio has no effect on the crystalline phase of the products, and all of the peaks corresponded well with the

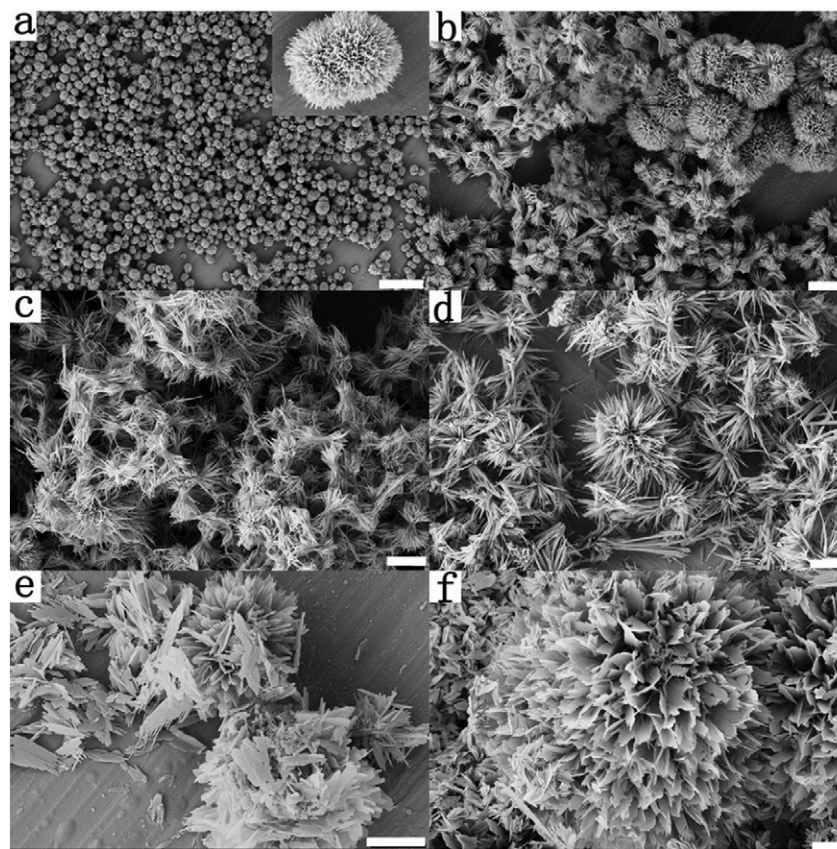


Fig. 1. SEM images of products obtained from different Ct/CTAB mole ratio condition. (a) 5/1, (b) 4/1, (c) 3/1, (d) 2/1, (e) 1/1 and (f) 1/0. The entire scale bar denotes 2 μm other than that in (a), which is 10 μm .

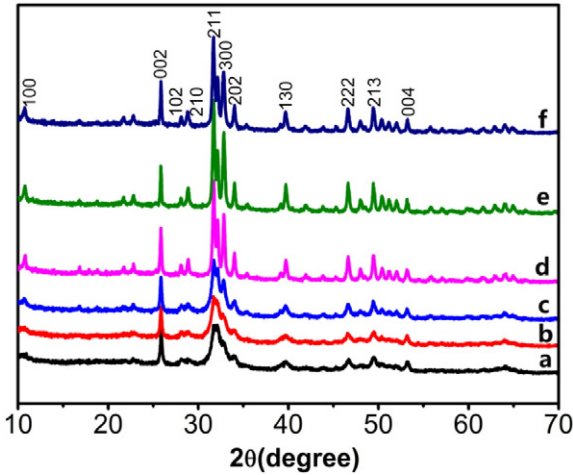


Fig. 2. XRD patterns of HAp particles obtained at different Ct/CTAB ratio. (a) 5/1, (b) 4/1, (c) 3/1, (d) 2/1, (e) 1/1 and (f) 1:0.

crystalline HAp ($P6_3/m$) and there was no other impurity that could be detected. Moreover, with the decreasing of Ct's concentration, the width of peaks between 30° to 35° became narrower, that indicated the crystallinity of the products improved. In vivo, citrate acid takes part in the process of biominerization and inhibits the crystallization of apatite [16]. Furthermore, citrate acid plays important role in restrain the formation of calculus [17]. Therefore, we believe sodium citrate might perform the same role, it suppressed the nucleation and growth of HAp at hydrothermal condition. Moreover, due to the high temperature and pressure, Ct would decomposed and generated acetonidicarboxylate complex, or even transformed into acetone and carbonate [18], which participated in the process of crystallization of HAp, and entered into crystal lattice. Numerous researches indicated introducing of carbonate had the following influence on HAp crystals: decrease the stability of crystalline structure; improve the crystal's dissolubility, and decrease crystallinity, that's consistent with our results [19].

Through FT-IR analysis (Fig. 3), we found that the composition among all of the samples was similar without any obvious difference, that's consistent with the XRD results. All spectra exhibit easily distinct and strong bands attributed to PO_4^{3-} groups. The characteristic spectra bands at around 1000 cm^{-1} were assigned to the components of the triply degenerated v_3 antisymmetric P-O stretching mode. The bands at around 500 cm^{-1} were ascribed to the doubly degenerate v_2 O-P-O bending mode [20]. The bands for C-H stretch in the range of $2750\text{--}3000 \text{ cm}^{-1}$ indicated that small amount of organic matters adsorbed onto the surface of samples. The broad band of low intensity in the range of $3200\text{--}3600 \text{ cm}^{-1}$ can be attributed to the traces of adsorbed water. Besides, the bands at around 1500 cm^{-1} indicated that small amount of CO_3^{2-} might be adsorbed onto the surface of particles, or even incorporated into the structure, its intensity was proportional to the concentration of Ct. After calcining, and the characteristic bands of PO_4^{3-} were not changed. However, the low density bands in the range of $1500\text{--}1750 \text{ cm}^{-1}$ demonstrated that CO_3^{2-} had two existence forms: incorporated into the HAp structure during the hydrothermal process, and adsorbed onto the surface of particles through electrostatic attraction.

CTAB is an effective surfactant for preparing HAp nanorods. In an aqueous system, CTAB ionizes completely and leads to the formation of cation with tetrahedral structure, the same with phosphate anion's structure. This charged structure and complementarity endows CTAB with the capability to control the crystallization process of HAp, these particles are nanoscale, but not microscale with orderly structure [21]. Hence, according to the results mentioned above, we speculate that Ct might play the following role.

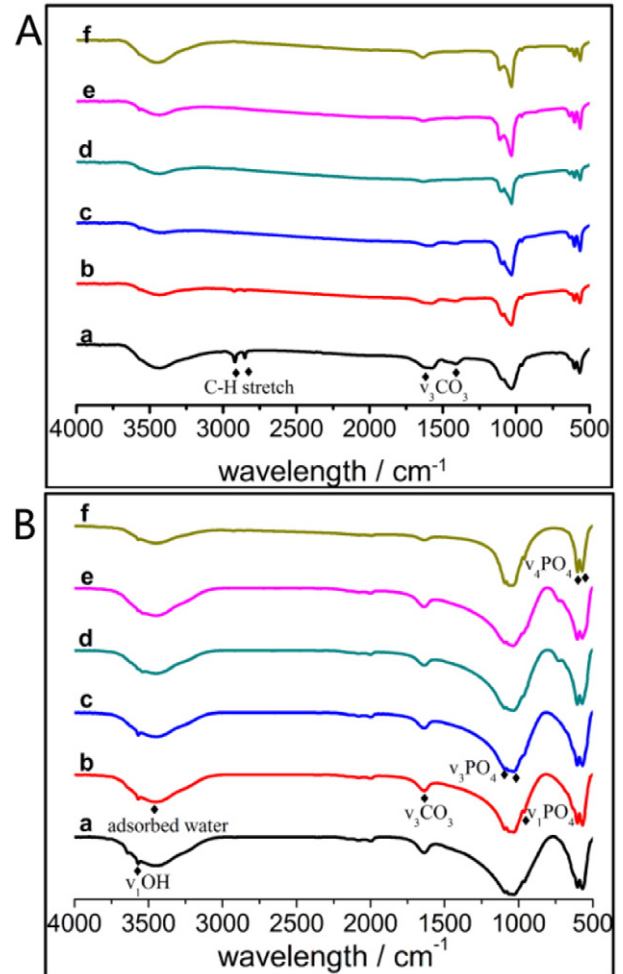


Fig. 3. FT-IR patterns of the as-prepared samples before (A) and after calcining at 1000°C (B). (a) 5/1, (b) 4/1, (c) 3/1, (d) 2/1, (e) 1/1 and (f) 1:0.

Firstly, it chelated Ca ions and formed CC, which provided nucleation sites for HAp. Besides, CC would be decomposed into Ca^{2+} and Ct^{3-} , then Ca^{2+} took part into the crystallization and growth process of HAp. Secondly, the specific adsorption of Ct at different crystal lattice planes of HAp led to crystals' heteroepitaxial growth along the c axis [22]. Meanwhile, Ct could modify the aggregation mode of crystals. High concentration of Ct not only accompanied with increased surface charge of crystals, but also prevented crystals' abnormal aggregation. Busch et al. studied anisotropic growth of FHAp by double diffusion technique in gelatin matrix, and successfully demonstrated its formation mechanism with a fractal model [23,24]. Besides, Yu-Ju Wu and co-workers synthesized FHAp with the aid of Ct, the fractal growth model was also a proper explanation for its formation process [25]. Herein, Ct might display the same role and led to the formation of sphere-like particles at high Ct concentration condition. The dipole field would be weakened when Ct concentration decreased, then affected the assemble mode of building blocks and resulted into the formation of nanoclusters. Moreover, slightly lowering the concentration of Ct is helpful for reducing the zeta potential of nanoparticles. Besides, the citrate molecules could be self-assembled by intermolecular hydrogen bond [16], then promoted an orderly aggregation behavior of nanocrystals along the c axis, that resulted the formation of laminar particles.

Except for the modifying agents and reactants' concentration, the initial status of crystal nucleus is closed related to the final structure, shape or even assemble fashion of building blocks [26]. Herein, a series of experiments were carried out, and results showed that the stirring

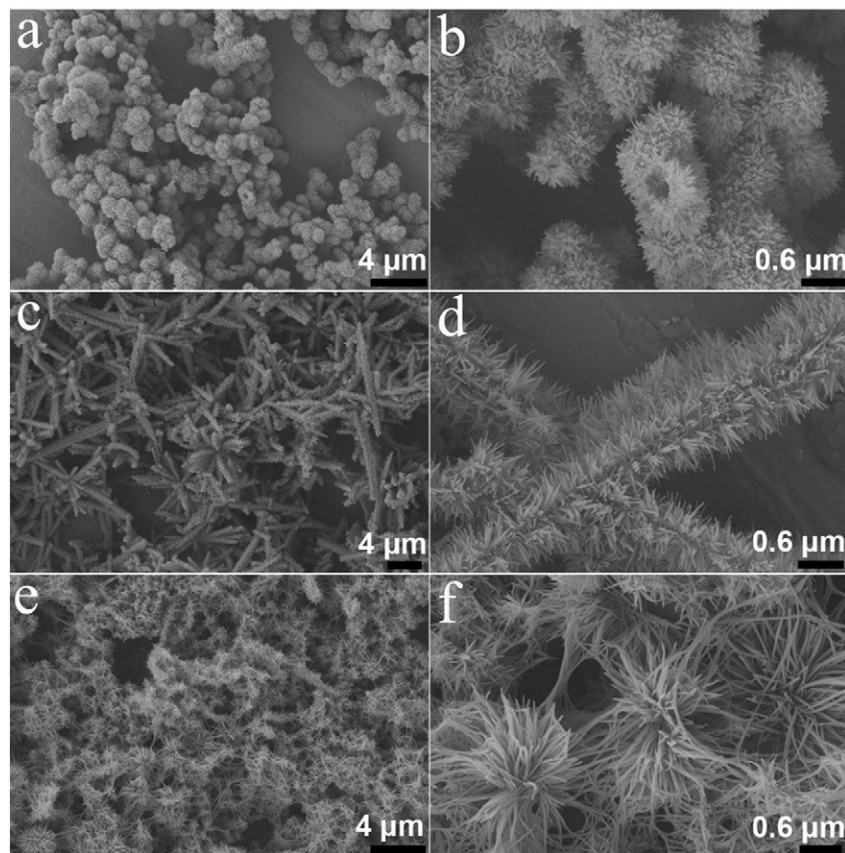


Fig. 4. SEM images of HAp obtained at different stirring time of Ca and Ct solution ($Ct/Ca = 3/1$). (a, b) 10 min; (c, d) 30 min; (e, f) 60 min. The length of the scale bars for (a, c, e) and (b, d, f) are 4 μm and 600 nm, respectively.

time of calcium citrate solution played an important role in regulating the final morphology of the crystals. In an aqueous system, citrate would chelate Ca^{2+} through its three carboxyl groups, and generated CC colloid nanoparticle clusters, these clusters were unstable and would further aggregate, that's why a clear solution containing Ca^{2+} and citrate became muddy after stirring for a while. Fig. 4 showed the morphology transformation of products at different stirring time condition. Short stirring time generated sphere-like particle with diameter ~600 nm (Fig. 4a, b). As building block, nanorod particles packed orderly and perpendicular to its surface. What's more, these spheres were not solid but contained an obvious cavity with the size about 100 nm.

Besides, because of the partially connected phenomenon of spheroid, worm-like particles with hollow hierarchical structure endowed the products with high specific surface area, and had the potential for the application of drug delivery. Increasing stirring time accompanied with the formation of bunched-like HAp microrod, which consisted of nanorod perpendicular to its center, and the center axis was quite different from the exterior structure, through calcining at 800 °C, we found that the center axis is empty (Fig. S1). When the stirring time was 60 min, the final products were HAp nanorod clusters, its building block was nanorod as well, while it's longer than that of the shorter stirring time group.

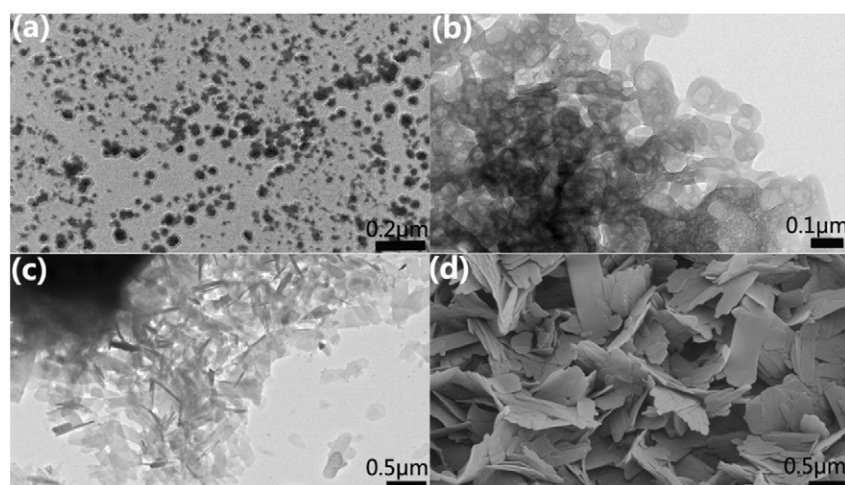


Fig. 5. TEM images of CC's shape transformation at different stirring time condition ($Ct/Ca = 3/1$). a 10 min, b 20 min, c 30 min, d 60 min.

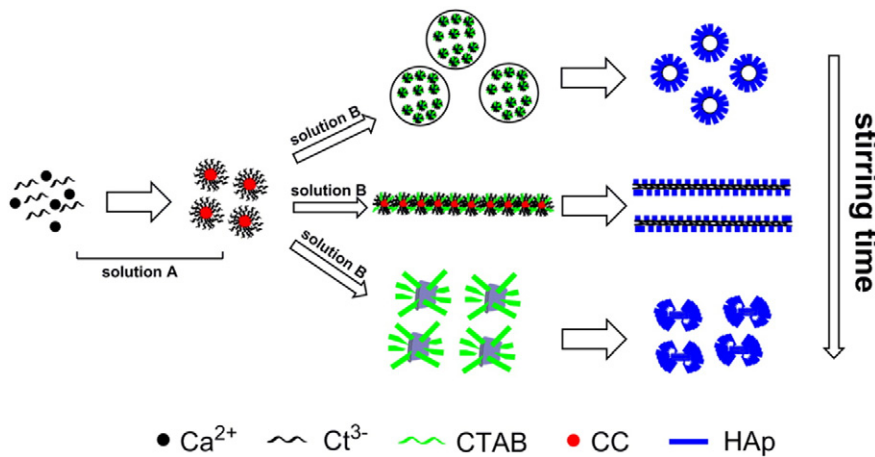


Fig. 6. Possible formation mechanism of HAp microcrystal with different hierarchical microstructure affected by CC's shape.

According to the results above, we speculated the morphology transformation of CC might be the key parameter in determining the microstructure of HAp crystals. Hence, the existence state evolution of CC was investigated (Fig. 5). At the initial stage, some dispersive tiny nanospheres were generated, and the size distribution was in the range of a few nanometers to tens of nanometers. Then these particles would further growing ($\sim 100\text{--}150\text{ nm}$), and aggregating phenomenon happened. Subsequently, sphere-like colloid particles disappeared, and then needle-/lamellar-like HAp crystals gradually formed. Because of their high surface energy, particles assembled orderly along their long axis, or parallel to their plane, that led to the formation of micro-lamellar particles with the size about $1\text{--}2\text{ }\mu\text{m}$.

Based on the investigation above, a plausible formation mechanism was proposed (Fig. 6). At an initial stage, CC nanoparticles/nano colloid particles formed, the mutual electrostatic repulsion endowed their dispersive status. These particles had the following roles: acted as template and provided nucleation sites for HAp; released Ca^{2+} slowly and then take part into the crystallization process of HAp. These nano-sized sphere-like particles determined the final diameter and shape of products. Meanwhile, relative slow decomposition rate caused the formation of hollow structure, besides, as CC tended to aggregate with each other, the final products were not dispersive but partially connected and formed worm-like crystals. As the stirring time increased, needle-like nanoparticles formed. Its high surface energy could be reduced through two modes: depositing HAp and parallel assembling along long axis, the former mode was beneficial for the formation of hierarchical structure, the rod-like building blocks were attributed to the modifying effect of CTAB, which caused a heterogeneity growth of HAp along the c axis through specific adsorption onto crystals' different lattice planes [27]. The later mode promoted the growth of microrod along long axis, and the decomposition of CC led to the formation of cavity structure along long axis of microrods. As the stirring time reached up to 120 min, the CC micro-lamellar with relatively high crystallinity generated, almost all of Ca^{2+} had been chelated with citrate, hence, the dissolution and decomposition rate of CC were controlled over the nucleation and growth speed of HAp directly, its relative high crystallinity meant quite slow Ca^{2+} releasing rate, that's why the cavity structure disappear in the final structure. Besides, micro-lamellar restricted the growth direction of HAp building blocks perpendicular to its surface, and caused the formation of nanorod clusters.

4. Conclusions

In summary, we have successfully synthesized HAp microcrystal with special hierarchical structures by controlling the solution reaction conditions, such as the mole ratio of Ct/CTAB, the stirring time of Ca–citrate solution. Citrate aggravates the orderly self-assemble of building

blocks, and CTAB modifying an oriented growth of HAp along the c axis. Besides, CC plays an important role in regulating the final structure of HAp particles. With the shape transformation of CC from sphere-like colloid, nano-needle to lamellar-like particles, the final products are hollow spheres, bunched-like microrods and nanorod clusters, respectively. The dissolution and decomposition rate of CC determine the formation of cavity structure.

Acknowledgment

This research was supported by Jiangxi University of Science and Technology Scientific Research Foundation (NSFJ2015-G11), Scientific Research Starting Foundation (jxxjbs14011) and Youth Science Foundation of Jiangxi Province (20151BAB216007).

Appendix A. Supplementary data

Supplementary data to this article can be found online at <http://dx.doi.org/10.1016/j.msec.2016.01.052>.

References

- [1] S.V. Dorozhkin, M. Epple, Biological and medical significance of calcium phosphates, *Angew. Chem. Int. Ed.* 41 (2002) 3130–3146.
- [2] T. Matsumoto, M. Okazaki, A. Nakahira, J. Sasaki, H. Egusa, T. Sohmura, Modification of apatite materials for bone tissue engineering and drug delivery carriers, *Curr. Med. Chem.* 14 (2007) 2726–2733.
- [3] B. Viswanath, N. Ravishankar, Controlled synthesis of plate-shaped hydroxyapatite and implications for the morphology of the apatite phase in bone, *Biomaterials* 29 (2008) 4855–4863.
- [4] J. Ryu, S.H. Ku, H. Lee, C.B. Park, Mussel-inspired polydopamine coating as a universal route to hydroxyapatite crystallization, *Adv. Funct. Mater.* 20 (2010) 2132–2139.
- [5] D.-M. Liu, T. Trocynski, W.J. Tseng, Water-based sol-gel synthesis of hydroxyapatite: process development, *Biomaterials* 22 (2001) 1721–1730.
- [6] M. Cao, Y. Wang, C. Guo, Y. Qi, C. Hu, Preparation of ultrahigh-aspect-ratio hydroxyapatite nanofibers in reverse micelles under hydrothermal conditions, *Langmuir* 20 (2004) 4784–4786.
- [7] B. Xie, G.H. Nancollas, How to control the size and morphology of apatite nanocrystals in bone, *Proc. Natl. Acad. Sci.* 107 (2010) 22369–22370.
- [8] K.S. Tenhuisen, R.I. Martin, M. Klimkiewicz, P.W. Brown, Formation and properties of a synthetic bone composite: hydroxyapatite–collagen, *J. Biomed. Mater. Res.* 29 (1995) 803–810.
- [9] P. Fratzl, H. Gupta, E. Paschalis, P. Roschger, Structure and mechanical quality of the collagen-mineral nano-composite in bone, *J. Mater. Chem.* 14 (2004) 2115–2123.
- [10] Y.-J. Wu, Y.-H. Tseng, J.C. Chan, Morphology control of fluorapatite crystallites by citrate ions, *Cryst. Growth Des.* 10 (2010) 4240–4242.
- [11] Y.-Y. Hu, A. Rawal, K. Schmidt-Rohr, Strongly bound citrate stabilizes the apatite nanocrystals in bone, *Proc. Natl. Acad. Sci.* 107 (2010) 22425–22429.
- [12] B. Nikooabkht, M.A. El-Sayed, Preparation and growth mechanism of gold nanorods (NRs) using seed-mediated growth method, *Chem. Mater.* 15 (2003) 1957–1962.
- [13] N.R. Jana, L. Gearheart, C.J. Murphy, Wet chemical synthesis of high aspect ratio cylindrical gold nanorods, *J. Phys. Chem. B* 105 (2001) 4065–4067.
- [14] C.J. Johnson, E. Dujardin, S.A. Davis, C.J. Murphy, S. Mann, Growth and form of gold nanorods prepared by seed-mediated, surfactant-directed synthesis, *J. Mater. Chem.* 12 (2002) 1765–1770.

- [15] K.R. Brown, D.G. Walter, M.J. Natan, Seeding of colloidal Au nanoparticle solutions. 2. Improved control of particle size and shape, *Chem. Mater.* 12 (2000) 306–313.
- [16] W. Jiang, H. Pan, Y. Cai, J. Tao, P. Liu, X. Xu, R. Tang, Atomic force microscopy reveals hydroxyapatite–citrate interfacial structure at the atomic level, *Langmuir* 24 (2008) 12446–12451.
- [17] W.O. Ekeruo, Y.H. Tan, M.D. Young, P. Dahm, M.E. Maloney, B.J. Mathias, D.M. Albala, G.M. Preminger, Metabolic risk factors and the impact of medical therapy on the management of nephrolithiasis in obese patients, *J. Urol.* 172 (2004) 159–163.
- [18] N. Gajbhiye, S. Prasad, Thermal decomposition of hexahydrated nickel iron citrate, *Thermochim. Acta* 285 (1996) 325–336.
- [19] J. Barralet, S. Best, W. Bonfield, Carbonate substitution in precipitated hydroxyapatite: an investigation into the effects of reaction temperature and bicarbonate ion concentration, *J. Biomed. Mater. Res.* 41 (1998) 79–86.
- [20] A. Ślōsarczyk, C. Palusziewicz, M. Gawlicki, Z. Paszkiewicz, The FTIR spectroscopy and QXRD studies of calcium phosphate based materials produced from the powder precursors with different CaP ratios, *Ceram. Int.* 23 (1997) 297–304.
- [21] Y. Wang, J. Chen, K. Wei, S. Zhang, X. Wang, Surfactant-assisted synthesis of hydroxyapatite particles, *Mater. Lett.* 60 (2006) 3227–3231.
- [22] H. Yang, L.J. Hao, N.R. Zhao, M.J. Huang, C. Du, Y.J. Wang, The growth process of regular radiated nanorod bundles hydroxyapatite formed by thermal aqueous solution approach, *Mater. Chem. Phys.* 141 (2013) 488–494.
- [23] R. Kniep, S. Busch, Biomimetic growth and self-assembly of fluorapatite aggregates by diffusion into denatured collagen matrices, *Angew. Chem. Int. Ed. Engl.* 35 (1996) 2624–2626.
- [24] P. Simon, D. Zahn, H. Lichte, R. Kniep, Intrinsic electric dipole fields and the induction of hierarchical form developments in fluorapatite–gelatine nanocomposites: a general principle for morphogenesis of biominerals? *Angew. Chem.* 118 (2006) 1945–1949.
- [25] Y.J. Wu, Y.H. Tseng, J.C.C. Chan, Morphology control of fluorapatite crystallites by citrate ions, *Cryst. Growth Des.* 10 (2010) 4240–4242.
- [26] D. Barreca, C. Massignan, S. Daolio, M. Fabrizio, C. Piccirillo, L. Armelao, E. Tondello, Composition and microstructure of cobalt oxide thin films obtained from a novel cobalt (II) precursor by chemical vapor deposition, *Chem. Mater.* 13 (2001) 588–593.
- [27] L. Yan, Y. Li, Z.X. Deng, J. Zhuang, X. Sun, Surfactant-assisted hydrothermal synthesis of hydroxyapatite nanorods, *Int. J. Inorg. Mater.* 3 (2001) 633–637.